IEEE Access
Multidisciplinary | Rapid Review | Open Access Journal

Received April 30, 2020, accepted May 12, 2020, date of publication May 26, 2020, date of current version June 8, 2020.

Digital Object Identifier 10.1109/ACCESS.2020.2997766

Dynamic Modeling and Residual Vibration Suppression of the Redundantly-Actuated Cable Driving Parallel Manipulator

ZHENGSHENG CHEN AND XUESONG WANG, (Member, IEEE)
Engineering Research Center of Intelligent Control for Underground Space, China University of Mining and Technology, Xuzhou 221116, China
School of Information and Control Engineering, China University of Mining and Technology, Xuzhou 221116, China

Corresponding author: Xuesong Wang (wangxuesongcumt@163.com)

This work was supported in part by the National Nature Science Foundation under Grant 61903347, and in part by the Natural Science Foundation of Zhejiang under Grant LY18E050019.

ABSTRACT An improved input shaping (IS) scheme was proposed for the redundantly actuated cable driving parallel robots (CDPRs) to suppress the residual vibration (RV). To make the design of the RV suppression convenient, the flexible displacements of the moving platform were taken as the generalized coordinates considering the axial deformation of cables, and rigid-flexible dynamic model of generalized redundantly actuated CDPRs was established with the Newton-Euler equation and the Newton's law. Then to cope with time-variant vibration frequencies of the CDPRs due to the variable lengths of cables, the technique that combined the one- to three-order zero vibration (ZV) IS with the particle swarm optimization (PSO) and the controller was proposed to suppress the RV. At last, to validate the effectiveness the proposed method, the simulations were carried out in a redundantly actuated CDPR that has six degree-of-freedom CDPR and seven driving cables with the proposed method, the results show that the RVs can be reduced significantly.

INDEX TERMS Cable-driving parallel manipulator robot, dynamic modeling, multiple mode input shaping, particle swarm optimization.

I. INTRODUCTION

Parallel manipulators have been an intensive area of research for over a decade and have been used in a wide spectrum of applications starting from simple pick and place operations of an industrial robot to advanced electronic manufacturing, maintenance of nuclear plants and space robotics [1], [2]. Due to the closed kinematic structures, parallel manipulators present better performance in accuracy, rigidity, and payload capacity and show greater potential to deal with these tasks [3].

Cable driving parallel robots(CDPRs) are an extension of traditional parallel manipulators by replacing rigid links with cables, which brings many advantages including a large workspace, low inertia links, cost-effective scalability, and potentially heavy payload capabilities [4]. However, the employing of the flexible cables also introduces two main disadvantages. On one hand, cables can only transmit pull forces, making it imperative that cables must remain in tension at all time to avoid out of control when in operation. A common approach for this problem is to introduce redundant branch to make the number of cables more than the number of the robot's degrees of freedom (DOF), which is called redundantly actuated CDPRs and the wrench can be controlled to make all cables in tension. On the other hand, cables usually exhibit more flexibility than the rigid links, which must cause severe residual vibration and would reduce the accuracy and efficiency especially for point-to-point motion. Hence, the residual vibration of the redundantly actuated CDPRs would be very essential for applications with many point-to-point motion.

Dynamic modeling is the basis for residual vibration, so an accurate and appropriate dynamic model for the redundantly actuated CDPRs is desirable. Existing dynamic modeling of the CDPRs mainly falls into two categories, which are rigid dynamic modeling and the rigid-flexible dynamic modeling. In the rigid dynamic modeling, the cables are tackled as massless rigid links, and the Lagrange equation or the Newton-Euler method are employed to establish the dynamic modeling of the moving platform [5], [6]. For the flexibility of the cables are neglected, the deformation or the vibration can't be taken into accounts and an accurate point-to-point

The associate editor coordinating the review of this manuscript and approving it for publication was Pedro Neto.

motion or trajectory tracking control would not be guaranteed. When the flexibility of cables is considered, the small deformation hypothesis is generally accepted. To obtain an accurate dynamic model, the transversal and axial deformation of cables are considered in [7], and the system dynamic model was obtained by eliminating redundant coordinates. While in most of other existing literature, the axial deformation was considered as the dominant component and the transversal deformation was neglected, then cables were modeled as massless axial spring and Newton-Euler equation was applied to establish the dynamic model of the moving platform, hence the system can be obtained from the force equilibrium, which is widely used in most literature for the accuracy and computation efficiency [4], [8], [9]. However, the flexible displacement of the CDPRs in this method was expressed as the difference of the desired and actual length of cables, an explicit expression of the flexible displacement of the moving platform was not given, which is an important variable in vibration suppression.

For the unique characteristics of the cable, many control methods for traditional flexible manipulators are not applicable to CDPRs, and the control method to deal with flexible CDPRs mainly falls into two categories: the feedback control and feedforward control. Among the feedback control, some researches neglected the flexibility of cables or perceived the flexibility as unknown lumped system dynamics [5], [10], [11]. Amir conducted continuous research on the vibration of the CDPR, an actuator configuration method was proposed to quantify the capacity of vibration suppression in all six DOFs over the kinematically constrained CDPR's workspace, and an optimal proportional-derivative (PD) controller was designed to minimize the maximum settling time of the vibration signals [12]. In [13], [14], the addition of two unbalanced-rotational-inertia actuators was introduced in the end-effector, and the sliding mode controller was applied to suppress the vibration for the CDPR. In [15], a new modeling and robust control approach was developed based on decoupling of nominal dynamics and vibration dynamics terms, and the trajectory tracking for the redundantly actuated CDPR was achieved by suppressing the vibration. Begey *et al.* [4] and Taghirad [16] and Shoaib *et al.* [17] adopt singular perturbation method to decompose the rigid-flexible dynamic model of the CDPRs into two subsystems, and the control scheme was designed for each subsystem respectively, which guarantee the stability of the control system and effectively suppress the vibration. To further improve the tracking accuracy, Caverly treated the sum of the flexible displacement and rigid-body motion as the control variable, then the passivity-based control scheme was employed to carry out trajectory tracking control [18], [19]. For the vibration and flexible deformation were all considered in the control design, the passivity-based redefinition method could obtain high trajectory tracking accuracy, of course the residual vibration can be suppressed.

Compared to the feedback control, feedforward-based vibration suppression algorithms do not require additional sensors or state feedback, so they are less expensive to implement. Feedforward control includes smooth basis function-based reference input method [20] and command shaping method [21]. Because the smooth function to construct the reference input method requires accurate dynamic models, the robustness is poor and the implementation process is more complicated, so the use of this method is limited. The command shaping is based on the system vibration characteristics to filter out the excitation components of the system from the reference input, which is relatively easy to implement. As the input shaping exhibits significantly better performance and easier implementation, it has important application potential and has been widely used attention.

The input shaping method involves a convolution operation on the original input signal and two pulses and applies the calculated signal to a second-order system to cancel the vibration which includes zero-vibration (ZV) shaper, the zero-vibration-derivative (ZVD) shaper and zero-vibration-derivative-derivative (ZVDD) shaper [21], [22]. The robustness to model errors is enhanced with the increase of the order of derivatives, but the time delay (TD) of the operation is also intensified. Existing literature shows that the IS technique could obtain satisfactory performance for linear time-invariant system. However, for time-variant system the CDPRs for example, cables in each branch have a different length in different position or posture, which means the time-variant stiffnesses and frequencies of the system. Researchers adopted time-variant input shapers, which need additional sensors for online measurement of the frequencies. Some researches employed the PSO to offline optimize the variable of the IS and get good RV suppression performance [23], [24]. But they didn't consider the controller and only perform one-order optimization.

In response to the above two issues, dynamic modeling and modified IS based RV suppression of the redundantly actuated CDPR will be carried out in this paper. In the dynamic modeling, flexible displacement of the moving platform will be selected as the generalized coordinates, and the deformation of the cables will be deduced from the Jaccobian matrix under the general accepted small deformation hypothesis, hence the dynamic model would be convenient for the residual vibration. Based on the proposed dynamic model, the modified IS that combined the multiple mode IS with the PSO and the feedforward plus PD control will be studied, unlike previous studies, the effectiveness of the technique will be given and the multi-mode IS will be carried out.

II. DYNAMIC MODELING OF THE GENERALIZED CDPR

As show in Fig.1, the m DOF generalized redundantly-actuated CDPR comprised of the base, the moving platform and n branches connected by cables. $\{O\}$ and $\{P\}$ coordinate frames are attached to the base and the moving platform with O and G, respectively, as the origins. The Cartesian coordinate vectors of points A_i and points B_i are denoted as $\mathbf{a}_i$ and $\mathbf{b}_i$ for $i = [1 \dots n]$, which are expressed in the moving platform frame and base frame, respectively.

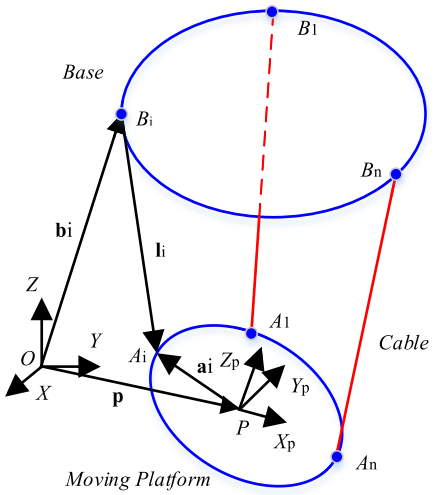

FIGURE 1. The structure of the CDPR.

$\mathbf{p}$ and $\mathbf{l}_\mathrm{i}$ represent the position of the moving platform and the cable in each branch. The pose $\boldsymbol{\eta} = [\mathbf{p}^\mathrm{T}\mathbf{o}^\mathrm{T}]^\mathrm{T}$ of the center of the moving platform P is composed of the position vector $\mathbf{p} = [x\ y\ z]^\mathrm{T}$ and the orientation vector $\mathbf{o} = [\phi\ \theta\ \varphi]^\mathrm{T}$, where Euler angles ϕ, θ and φ are orientations about X-, Y- and Z- axes respectively, and the rotation matrix is calculated as,

$$\mathbf{R}_p = \mathbf{R}_z(\phi)\mathbf{R}_y(\theta)\mathbf{R}_x(\varphi) \tag{1}$$

Then, the motion equation and the length of the ith cable is expressed as,

$$\begin{cases} \mathbf{l}_i = \mathbf{p} - \mathbf{b}_i + \mathbf{R}_p\mathbf{a}_i \\ l_i = \|\mathbf{l}_i\| = \sqrt{\left(\mathbf{p} - \mathbf{b}_i + \mathbf{R}_p\mathbf{a}_i\right)^\mathrm{T}\left(\mathbf{p} - \mathbf{b}_i + \mathbf{R}_p\mathbf{a}_i\right)} \end{cases} \tag{2}$$

where $\mathbf{l}_i$ and l_i are the vector and length of the ith cable respectively. Take the derivative of the first equation of (2) and take dot multiplication with $\mathbf{d}_i = \mathbf{l}_i/l_i$, the unit vector of the cable, we have,

$$\begin{cases} \dot{\mathbf{l}} = \left[\dot{l}_1;\cdots;\dot{l}_\mathrm{n}\right] = \mathbf{J}\left[\dot{\mathbf{p}};\boldsymbol{\omega}\right] = \mathbf{J}\mathbf{S}'\left[\dot{\mathbf{p}};\dot{\mathbf{o}}\right] \\ \mathbf{J} = \begin{bmatrix} \mathbf{d}_1 & \cdots & \mathbf{d}_\mathrm{n} \\ \mathbf{R}_p\mathbf{a}_1 \times \mathbf{d}_1 & \cdots & \mathbf{R}_p\mathbf{a}_\mathrm{n} \times \mathbf{d}_\mathrm{n} \end{bmatrix}^\mathrm{T} \end{cases} \tag{3}$$

where a dot means derivative, $\dot{\mathbf{l}}$ represents the vector of velocity of the length of all cables, $\dot{\mathbf{p}}$ and $\dot{\mathbf{o}}$ are the derivative of $\dot{\mathbf{p}}$ and $\dot{\mathbf{o}}$ respectively, $\mathbf{J}$ is the Jaccobian matrix depicting the velocity mapping between the moving platform and cables, and $\boldsymbol{\omega} = \mathbf{S}\dot{\mathbf{o}}$ represents the angular velocity of the moving platform with respect to the base frame. The mapping matrix $\mathbf{S}'$ and unit matrix $\mathbf{S}$ can be given as,

$$\mathbf{S}' = \begin{bmatrix} \mathbf{I}_{3\times3} & \mathbf{0}_{3\times3} \\ \mathbf{0}_{3\times3} & \mathbf{S} \end{bmatrix}, \quad \mathbf{S} = \begin{bmatrix} 0 & -\sin\phi & \cos\phi\cos\theta \\ 0 & \cos\phi & \cos\theta\sin\phi \\ 1 & 0 & -\sin\theta \end{bmatrix} \tag{4}$$

According to most existing literature, the axial deformation is dominant, and the stiffness of the ith cable is expressed as,

$$k_i = EA/l_i \tag{5}$$

where E and A are the Young modulus of elasticity and the cross area of cables, respectively.

Unlike previous papers which takes the deformation of cables as the generalized coordinates, the flexible displacement of the moving platform will take the place in this paper to make the dynamic model convenient for the vibration suppression, and the flexible displacement are denoted as $\delta\boldsymbol{\eta} = [\delta\mathbf{p}^\mathrm{T}\quad \delta\mathbf{o}^\mathrm{T}]^\mathrm{T}$. Hence, under the small deformation hypothesis, the deformation of all cables can be obtained as,

$$\delta\mathbf{l} = \mathbf{J}\mathbf{S}'\left[\delta\mathbf{p}^\mathrm{T}\quad \delta\mathbf{o}^\mathrm{T}\right]^\mathrm{T} \tag{6}$$

Considering the flexibility of cables, the dynamic model of the moving platform using the Newton-Euler method can be given as,

$$\begin{aligned} &\begin{bmatrix} m_p\mathbf{I}_{3\times3} & \mathbf{0}_{3\times3} \\ \mathbf{0}_{3\times3} & \mathbf{S}^\mathrm{T}\mathbf{R}_p^\mathrm{T}\mathbf{I}_p\mathbf{R}_p\mathbf{S} \end{bmatrix}(\ddot{\boldsymbol{\eta}} \\ &+\delta\ddot{\boldsymbol{\eta}}) + \begin{bmatrix} \mathbf{0}_{3\times1} \\ \mathbf{S}^\mathrm{T}\Big(\mathbf{S}\left(\dot{\mathbf{o}}+\delta\dot{\mathbf{o}}\right)\times\mathbf{R}_p^\mathrm{T}\mathbf{I}_p\mathbf{R}_p\mathbf{S} + \\ \mathbf{R}_p^\mathrm{T}\mathbf{I}_p\mathbf{R}_p\dot{\mathbf{S}}\Big)\left(\dot{\mathbf{o}}+\delta\dot{\mathbf{o}}\right) \end{bmatrix} = -\mathbf{S}'^\mathrm{T}\mathbf{J}^\mathrm{T}\mathbf{K}\delta\mathbf{l} + m_p\begin{bmatrix} \mathbf{g} \\ \mathbf{0}_{3\times3} \end{bmatrix} \end{aligned} \tag{7}$$

where m_p is the mass of the moving platform, $\mathbf{I}_p$ is the rotational inertial with respect to the body-fixed coordinate frame, and $\mathbf{K} = \mathbf{diag}\left([k_1\cdots k_\mathrm{n}]\right)$ is the stiffness matrix. The dynamic model of pulleys near the motor can be expressed,

$$I_b\ddot{\boldsymbol{q}} = \boldsymbol{\tau} + r\mathbf{K}\delta\mathbf{l} \tag{8}$$

where I_b and r are the rotational inertial and radius of the pulleys, and $\ddot{\mathbf{q}}$ represent the corresponding angular acceleration, which can be expressed from equation (3),

$$\ddot{\mathbf{q}} = \ddot{\mathbf{l}}/r = \left(\mathbf{J}\mathbf{S}'\ddot{\boldsymbol{\eta}} + \mathbf{J}\dot{\mathbf{S}}'\dot{\boldsymbol{\eta}} + \dot{\mathbf{J}}\mathbf{S}'\dot{\boldsymbol{\eta}}\right)/r \tag{9}$$

Substitute (9) into (8), and divide by r and multiply $\mathbf{S}'\mathbf{J}^\mathrm{T}$ for both sides of the new equation, which is added up with (7), then the dynamic model of the CDPR can be given as,

$$\mathbf{M}\begin{bmatrix} \ddot{\boldsymbol{\eta}} \\ \delta\ddot{\boldsymbol{\eta}} \end{bmatrix} + \mathbf{f} + \begin{bmatrix} \mathbf{0}_{6\times1} \\ \mathbf{S}'^\mathrm{T}\mathbf{J}^\mathrm{T}\mathbf{K}\mathbf{J}\mathbf{S}'\delta\boldsymbol{\eta} \end{bmatrix} = \begin{bmatrix} \mathbf{S}'\mathbf{J}^\mathrm{T}\boldsymbol{\tau}/r \\ \mathbf{0}_{6\times1} \end{bmatrix} \tag{10}$$

where

$$\begin{aligned} \mathbf{f} &= \begin{bmatrix} \mathbf{f}_0 + I_b\mathbf{S}'^\mathrm{T}\mathbf{J}^\mathrm{T}\left(J\dot{\mathbf{S}}'\dot{\boldsymbol{\eta}} + \dot{\mathbf{J}}\mathbf{S}'\dot{\boldsymbol{\eta}}\right)/r^2 \\ \mathbf{f}_0 \end{bmatrix}, \\ \mathbf{M} &= \begin{bmatrix} \mathbf{M}_{11} & \mathbf{M}_{22} \\ \mathbf{M}_{22}^\mathrm{T} & \mathbf{M}_{22} \end{bmatrix}, \\ \mathbf{M}_{22} &= \begin{bmatrix} m_p\mathbf{I}_{3\times3} & \mathbf{0}_{3\times3} \\ \mathbf{0}_{3\times3} & \mathbf{S}^\mathrm{T}\mathbf{R}_p^\mathrm{T}\mathbf{I}_p\mathbf{R}_p\mathbf{S} \end{bmatrix}, \\ \mathbf{M}_{11} &= \mathbf{M}_{22} + I_b\mathbf{S}'^\mathrm{T}\mathbf{J}^\mathrm{T}\mathbf{J}\mathbf{S}'/r^2, \\ \mathbf{f}_0 &= \begin{bmatrix} -\mathbf{G}_\mathrm{p} \\ \mathbf{S}^\mathrm{T}\Big(\mathbf{S}\left(\dot{\mathbf{o}}+\delta\dot{\mathbf{o}}\right)\times\mathbf{R}_p^\mathrm{T}\mathbf{I}_p\mathbf{R}_p\mathbf{S} + \mathbf{R}_p^\mathrm{T}\mathbf{I}_p\mathbf{R}_p\dot{\mathbf{S}}\Big)\left(\dot{\mathbf{o}}+\delta\dot{\mathbf{o}}\right) \end{bmatrix} \end{aligned}$$

Since the number of the driving cables n is more than the number of the DOF m in the redundantly actuated CDPRs,

from (7) the cable tensions of the redundantly actuated CDPR can be calculated as,

$$\mathbf{F} = -\mathbf{W}^{+}\left(\mathbf{M}_{22}\left(\ddot{\boldsymbol{\eta}} + \delta\ddot{\boldsymbol{\eta}}\right) + \mathbf{f}_0\right) - \mathbf{N}\lambda \tag{11}$$

where $\mathbf{W}^{+} = \mathbf{W}^{\mathrm{T}}\left(\mathbf{W}\mathbf{W}^{\mathrm{T}}\right)^{-1}$ is the Moore–Penrose of $\mathbf{W} = \mathbf{S}'^{\mathrm{T}}\mathbf{J}^{\mathrm{T}}$, $\mathbf{N} = \ker(\mathbf{W})$ is the matrix of null space basis unit vectors of $\mathbf{W}$, and $\boldsymbol{\lambda}$ is (n-m) dimension arbitrary vector. It should be noted that (11) represents all the possible solutions for the cables' tensions. For the given pose of the moving platform, the driving torques $\boldsymbol{\tau}$ should be definite and energy-saving, hence in this study, the 2-norm optimal tension of the cables is defined as the optimization objective. From Equation (10), without considering the cable tension, the nominal control torques $\boldsymbol{\tau}_{\mathrm{nom}} = \mathbf{W}^{+}\mathbf{F}_{\mathrm{nom}}$ is valid, and 2-norm of the torques when considering the tensions can be written as,

$$\boldsymbol{\tau}^{\mathrm{T}}\boldsymbol{\tau} = \left(\mathbf{W}^{+}\mathbf{F}_{\mathrm{nom}} + \mathbf{N}\lambda\right)^{\mathrm{T}}\left(\mathbf{W}^{+}\mathbf{F}_{\mathrm{nom}} + \mathbf{N}\lambda\right) = \boldsymbol{\lambda}^{\mathrm{T}}\boldsymbol{\lambda}$$

Considering the positive range for the cables and energy-saving, the positive tensions can be obtained by solving the following quadratic programming,

$$\begin{aligned} &\min\ \boldsymbol{\lambda}^{\mathrm{T}}\boldsymbol{\lambda} \\ &\text{subject to}\ -\mathbf{W}^{+}\left(\mathbf{M}_{22}\left(\ddot{\boldsymbol{\eta}} + \delta\ddot{\boldsymbol{\eta}}\right) + \mathbf{f}_0\right) - \mathbf{N}\lambda - \mathbf{F}_{\delta} \geq 0 \end{aligned} \tag{12}$$

where $\mathbf{F}_{\delta}$ is the selected positive vector to keep redundancy in positive tension.

III. RV WITH MODIFIED MULTIPLE MODE IS

A. RV SUPPRESSION PRINCIPLE WITH MULTIPLE MODE IS

Input shaping is the process of convolving the original input signal with the pulse signal to obtain a new signal, the vibration suppression based on which splits the input signal into multiple signals according to the characteristics of the periodic response of the dynamic system, and the vibration is eliminated by superposing the response. Take the two pulses shaping shown in Fig.2 as an example, Fig.2 (a) shows the initial signal and the shaped two pulses, which can be obtained by convolution operation. Fig.2 (b) gives the response of the shaped pulses A_{p1} and A_{p2}, from which we can conclude that the superposing response can be zero by selecting properly parameters of the pulse.

For a second-order underdamped system, when a pulse with the intensity A_{pi} takes effect at time t_i, the response of which can be expressed as,

$$y_i(t) = \frac{A_{pi}\omega_n}{\sqrt{1-\xi^2}} e^{-\xi\omega_n(t-t_i)} \sin\left(\omega_n\sqrt{1-\xi^2}(t-t_i)\right) \tag{13}$$

where ξ is linear damping, ω_n is the natural frequency of the system.

According to the principle of superposition of linear systems, the system response under the action of n_p pulse can be expressed as,

$$y(t) = B_t \sin\left(\omega_n\sqrt{1-\xi^2}t + \gamma\right) \tag{14}$$

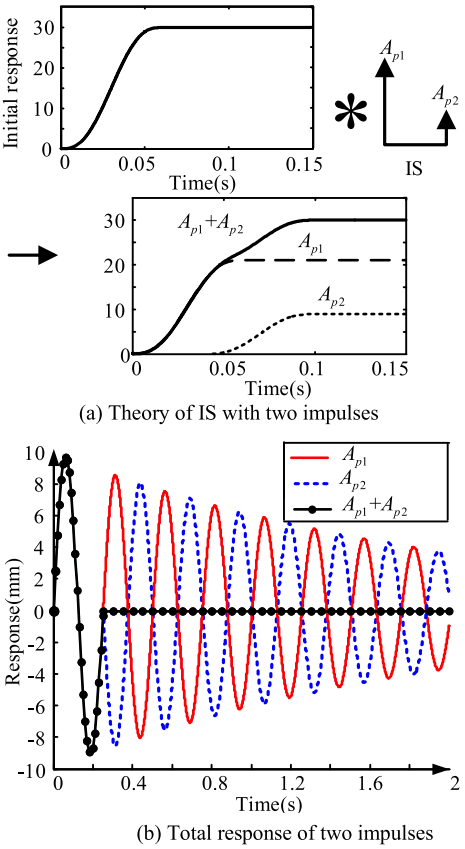

(a) Theory of IS with two impulses

(b) Total response of two impulses

FIGURE 2. Basic theory of input shaping.

where

$$B_t = \sqrt{\left(\sum_{i=1}^{n_p} B_{ti}\cos\left(\omega_d t_i\right)\right)^2 + \left(\sum_{i=1}^{n_p} B_{ti}\sin\left(\omega_d t_i\right)\right)^2},$$

$$\gamma = \tan^{-1}\left(\sum_{i=1}^{n_p}\frac{B_{ti}\cos\left(\omega_d t_i\right)}{B_{ti}\sin\left(\omega_d t_i\right)}\right), \quad \omega_d = \omega_n\sqrt{1-\xi^2},$$

$$B_{ti} = \frac{A_{pi}\omega}{\sqrt{1-\xi^2}} e^{-\xi\omega_n(t-t_i)}$$

If we expect the system's residual vibration completely suppressed after the time t_{n_p}, the amplitude of the system's multi-pulse response at time t_{n_p} should satisfy $B_t = 0$, we have,

$$\begin{cases} \sum_{i=1}^{n_p} \frac{A_{pi}\omega_n}{\sqrt{1-\xi^2}} e^{-\xi\omega_n\left(t_{n_p}-t_i\right)} \cos\left(\frac{\omega_n t_i}{\sqrt{1-\xi^2}}\right) = 0 \\ \sum_{i=1}^{n_p} \frac{A_{pi}\omega_n}{\sqrt{1-\xi^2}} e^{-\xi\omega_n\left(t_{n_p}-t_i\right)} \sin\left(\frac{\omega_n t_i}{\sqrt{1-\xi^2}}\right) = 0 \end{cases} \tag{15}$$

To guarantee the CDPRs reach the expected position or orientation, the intensity of the summed pulses should be the unit, so the following equation should be validated,

$$\sum_{i=1}^{n_p} A_{pi} = 1 \tag{16}$$

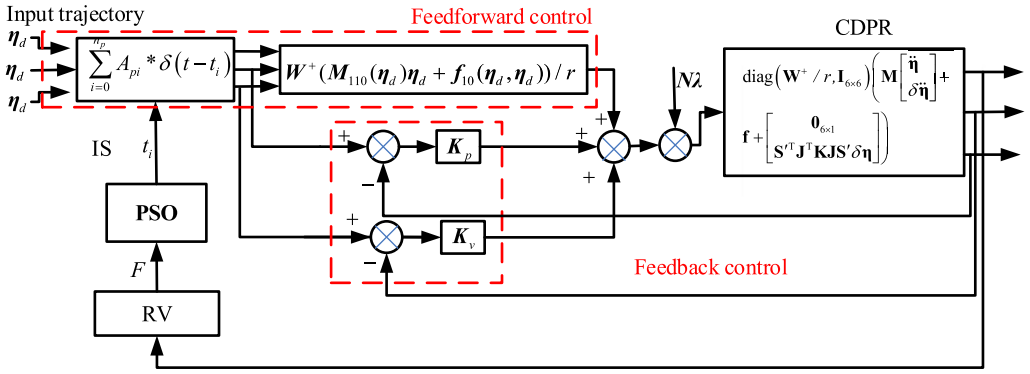

FIGURE 3. Multiple-mode IS and PSO based trajectory planning.

From (4) and (5), the intensity of the two pulses and the corresponding moment of action are expressed as,

$$\begin{cases} \begin{bmatrix} \mathbf{A}_{p1} \\ \mathbf{t}_1 \end{bmatrix} = \begin{bmatrix} A_{p11} & A_{p12} \\ 0 & t_{11} \end{bmatrix}; \; K_t = e^{-\frac{\xi\pi}{\sqrt{1-\xi^2}}}; \; A_{p11} = \dfrac{1}{1+K_t}; \\ t_{11} = \pi/\omega_n\sqrt{1-\xi^2}; \quad A_{p12} = \dfrac{K_t}{1+K_t} \end{cases} \tag{17}$$

The cascade method and combination method are mainly used to achieve the vibration suppression of multi-order IS, and the former method would be adopted in this paper for the advantages of high robustness and easy implementation. Similarly, the second- and third-order shaper parameters can be expressed as [25], (18) and (19), as shown at the bottom of this page.

B. THE PROPOSAL OF THE MODIFIED IS

From the principle of the IS, we can see that traditional IS can only suppress RV for systems with time-invariant frequencies. However, the frequencies of the redundantly-actuated CDPRs will be time-variant when operating in different poses, and the RV will be the implicit periodic responses which is the superpositions of the sine functions including all the time-variant frequencies, hence the traditional IS will not work for frequencies of the periodic responses can't be explicit calculated.

For every periodic function can be approximated by the sine functions, in order to suppress the residual vibration of the CDPRs, the multiple-mode IS is combined with the PSO and dynamic feedforward plus PD control in this paper. The shaping position of the multiple-mode IS is used as the optimization variable, and the summed residual vibration of all cables is used as the optimization objective. The entire optimization process is shown in Fig.3, with the shaper position as the optimization variable, the PSO generates a population for each optimization variable, which will be applied in IS and calculated in the corresponding summed residual vibration F as the fitness function. The PSO would search the minimum value of F until the requirements are met, where n_p is the number of shapers, $\delta(t-t_i)$ is the pulse at the moment t_i, and A_{pi} is the pulse amplitude.

For the moving platform usually possess translational and rotational motions which are of different measures, the maximal mean squared summed residual vibration of all cables after 1 second of the movement was selected as the optimization objective, which can be expressed as,

$$F = \min_{t\in S}(\sqrt{\max(\delta\boldsymbol{\eta}^{\mathrm{T}}\mathbf{S}'^{\mathrm{T}}\mathbf{J}^{\mathrm{T}}\mathbf{J}\mathbf{S}'\delta\boldsymbol{\eta})}), \quad (S: t_d \le t \le t_d+1) \tag{20}$$

C. THE PROCESS OF THE MODIFIED IS

PSO, proposed by Kennedy, is an iterative evolutionary algorithm based on bird foraging, in which particles follow the optimal particles to search in the solution space without the need for crossover and mutation operations in genetic algorithm, and requires less computational cost and parameters adjustment, so it has been widely used [20]. For the time-variant frequencies of the redundantly actuated CDPRs in different pose, the PSO will be employed to optimize the input shapers to obtain the minimum residual vibration. According to Fig.3, the entire optimization process is as follows,

(1) Initialize the number of iterations $k = 1$ and randomly initialize N_p positions and flying velocities with

$$\begin{bmatrix} \mathbf{A}_{p2} \\ \mathbf{t}_2 \end{bmatrix} = \begin{bmatrix} A_{p11}A_{p21} & A_{p11}A_{p22} & A_{p12}A_{p21} & A_{p21}A_{p22} \\ 0 & t_{11} & t_{11}+t_{21} & t_{11}+t_{21} \end{bmatrix} \tag{18}$$

$$\begin{bmatrix} \mathbf{A}_{p3} \\ \mathbf{t}_3 \end{bmatrix} = \begin{bmatrix} A_{p11}A_{p21}A_{p31} & A_{p11}A_{p22}A_{p31} & A_{p12}A_{p21}A_{p31} & A_{p21}A_{p22}A_{p31} \\ 0 & t_{11} & t_{11}+t_{21} & t_{11}+t_{21} \\ A_{p11}A_{p21}A_{p32} & A_{p11}A_{p22}A_{p32} & A_{p12}A_{p21}A_{p32} & A_{p21}A_{p22}A_{p32} \\ t_{31} & t_{11}+t_{31} & t_{11}+t_{21}+t_{31} & t_{11}+t_{21}+t_{31} \end{bmatrix} \tag{19}$$

n_p dimensions in solution space dimension, ($n_p = 1, 2, 3$), which can be expressed as,

$$\mathbf{x}_i^k = \left[x_{1,i}, x_{2,i} \cdots, x_{Np,i}\right], \quad \mathbf{v}_i^k = \left[v_{1,i}, v_{2,i} \cdots, v_{Np,i}\right], \quad i = 1 \ldots n_p \tag{21}$$

(2) Substitute the position of each particle into the IS's time variable to shape the desired trajectory, and the fourth-order Runge-Kutta method was employed to calculate the real rigid and flexible displacements of the redundantly actuated CDPR controlled by dynamic feedforward plus PD control and the quadratic-programming based $\mathbf{N}\lambda$ to guarantee positive cable tension, the values of which at the final moment was applied as the input to calculate the maximum value of the residual vibration within 1s after operation, which is the fitness function of each particle $F_j^k, j = 1, 2, \ldots, m_p$. Then initialize the particle positions $\mathbf{pb}_i$ of the fitness function of local optimal, which is particle position $\mathbf{gb}$ of the optimal value in the last iteration and the global optimal value.

(3) Positions and flying velocities of particles are updated as followings,

$$\begin{cases} \mathbf{v}_i^{k+1} = \gamma_0 \left[\mathbf{v}_i^{k+1} + p_1 r_1^k \left(\mathbf{pb}_i - \mathbf{x}_i^k\right) + p_2 r_2^k \left(\mathbf{gb} - \mathbf{x}_i^k\right)\right] \\ \mathbf{x}_i^{k+1} = \mathbf{x}_i^k + \mathbf{v}_i^{k+1} \end{cases} \tag{22}$$

where r_1^k and r_2^k are random value between 0 and 1, p_1 and p_2 are set to 2.05, and γ_0 is defined as,

$$\gamma_0 = \frac{2}{\left|2 - (p_1 + p_2) - \sqrt{(p_1 + p_2)^2 - 4(p_1 + p_2)}\right|} \tag{23}$$

(4) Calculate the fitness function value corresponding to each particle. Update the particle position corresponding to the local optimal value and the global optimal value. If the fitness value of the current function is greater than the local optimal value, update $\mathbf{pb}_i$ to the current position. If the fitness function corresponding to all particles is greater than the global optimal value, update $\mathbf{gb}$ to particle position of the optimal fitness function value.

(5) If current iteration step satisfy $k < K_{\max}$ and the tolerance of the fitness function $TolFun > \varepsilon_d$, set $k = k+1$ and repeat the steps (3) to (5), otherwise, output $\mathbf{gb}$ and its corresponding fitness value.

IV. CASE STUDY

To validate the proposed RV suppression method for the redundantly actuated CDPR, the six DOF CDPR with 7 driving cables as shown in Fig.4 will be taken as example in the simulation. The dimensions and mechanical properties are given in TABLE 1 and TABLE 2.

In order to verify the proposed algorithm, the fifth-order polynomial depicting the point-to-point motion as shown in (24) is used for the simulation, and parameters of one- to three- order IS will be optimized to suppress the residual vibration, and set the maximum iteration step $K_{\max} = 300$,

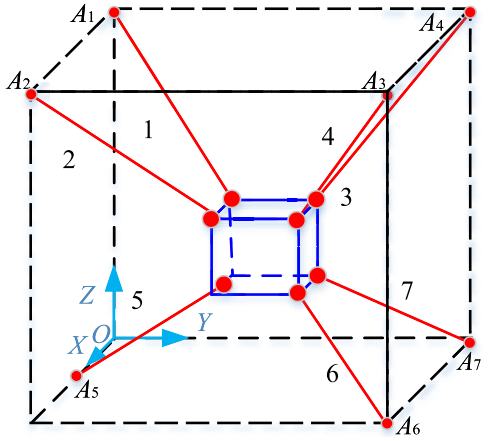

FIGURE 4. Six-DOF CDPR with seven cables.

TABLE 1. Dimension of the CDPR (in mm).

Dimension	Value	Dimension	Value
$\mathbf{b}_1$	[0,0,1000]	$\mathbf{a}_1$	[-150,-100,50]
$\mathbf{b}_2$	[100,0,1000]	$\mathbf{a}_2$	[150,-100,50]
$\mathbf{b}_3$	[1000,1000,1000]	$\mathbf{a}_3$	[150,100,50]
$\mathbf{b}_4$	[0,1000,1000]	$\mathbf{a}_4$	[-150,100,50]
$\mathbf{b}_5$	[500,0,0]	$\mathbf{a}_5$	[0,-100,-50]
$\mathbf{b}_6$	[1000,1000,0]	$\mathbf{a}_6$	[150,100,-50]
$\mathbf{b}_7$	[0,1000,0]	$\mathbf{a}_7$	[-150,100,50]
r	40		

TABLE 2. Mechanical properties of the CDPR.

Parameter	Description	Value
E	Young modulus of elasticity of cables	210GPa
A	Cross section area of cables	3.14mm^2
m_p	mass of the MP	66.7kg
$\mathbf{I}_p$	rotational inertia matrix of the MP	**diag**(1.1×10^6, 2.2×10^6, 2.9×10^6) (kg•mm^2)
I_b	rotational inertia of the pulley	

TABLE 3. The optimized parameters and performance with different ISs.

Number of IS	time t_{11}(s)	Time t_{21}(s)	Time t_{31}(s)	TD (s)	RV (mm)
No IS	—	—	—	0	0.037
One IS	0.0896	—	—	0.0896	0.011
Two ISs	0.0869	0.0528	—	0.1397	0.0021
Three ISs	0.0895	0.0736	0.0185	0.1816	0.00063

the tolerance of the fitness function $TolFun = 1 \times 10^{-6}$, and the number of particles $N_p = 40$ for the PSO.

$$\begin{cases} x = 20\left(6t^5/t_d^5 - 15t^4/t_d^4 + 10t^3/t_d^3\right) + 450 \\ y = 700; \quad z = 500; \ \phi = \theta = \varphi = 0 \end{cases} \tag{24}$$

where $t_d = 0.2$ s. The optimization results are shown in TABLE 3, we can see that without the IS, the maximum RV of cables are 0.037mm, and corresponding value is suppressed to 0.011mm when one-order IS is used, about 70% RV is eliminated. Further, when two- and three-order IS

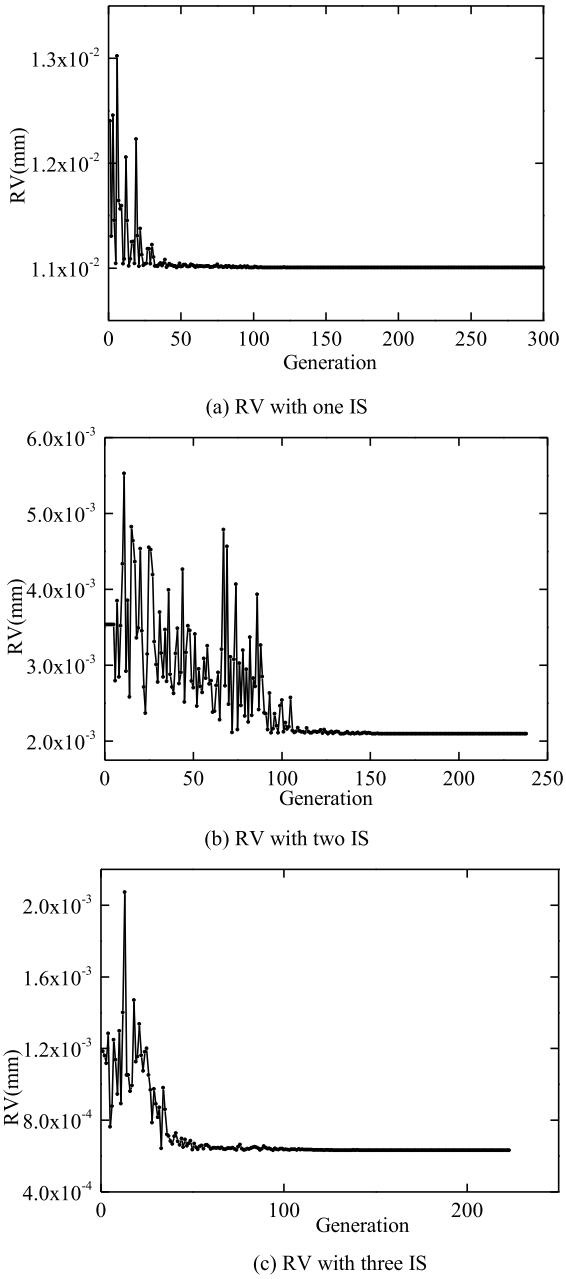

FIGURE 5. Results of RV with different shapers.

was employed for the optimization, the IS was reduced to 0.0021mm and 0.00063mm, respectively, approximately 94% and 98% RV are suppressed, which means that the proposed method could effectively suppress the RV. Also, we should note that when the IS is used, the time delay is induced, the magnitude of which depends on the low-order vibration frequencies of the system, and the time delay becomes larger with the increase of the order of the IS. The time delay and the performance of the RV should be balanced in different industrial application, in generalized applications, one- or two-order IS would satisfy the accuracy requirements while the time delay is acceptable, but for applications requiring high or ultra-high accuracy, the three-or even higher order IS might be demanded.

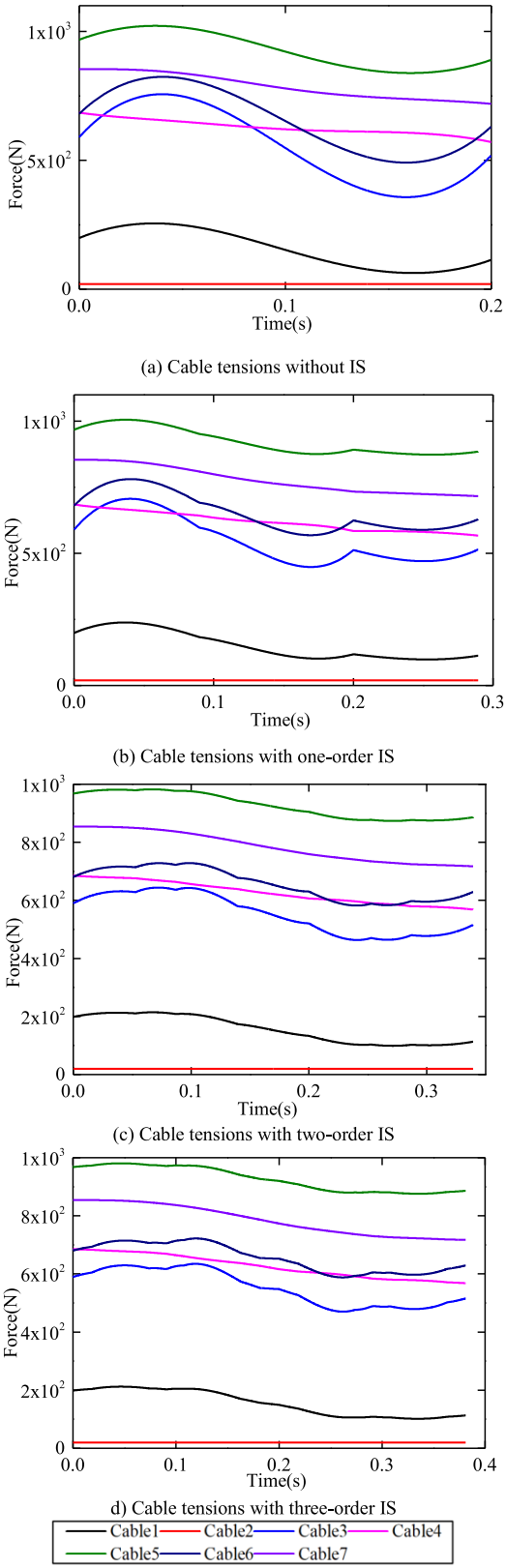

FIGURE 6. Cable tensions with different IS.

In the optimization, the $\mathbf{F}_\delta$ is set 20N, the cable tensions are calculated according to Fig.3 and the quadratic programming expressed in Equation (12), the results are shown in Fig.6.

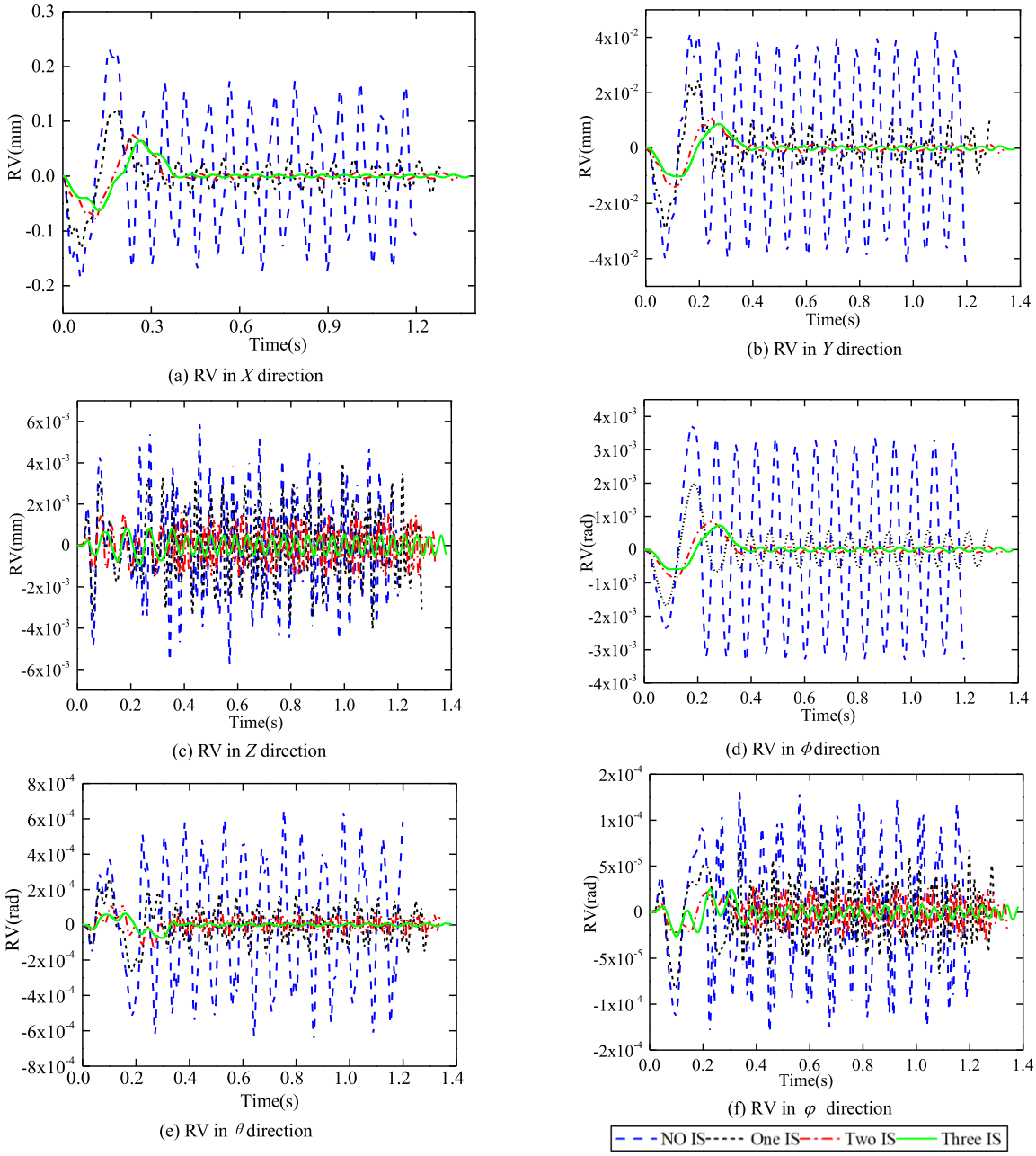

FIGURE 7. Flexible displacement of the moving platform with different IS.

We can see that all the cable tensions are positive when operating with different IS, and the minimum value are near $\mathbf{F}_\delta$, which implies that the constraint in the optimization is satisfied. Also, maximum cable tensions are reduced with the increase of the number of the IS, which is caused by the increasing time delay induced by the IS. Therefore, we can conclude that the cable positive tensions can be guaranteed in the RV with the multiple-mode IS.

From the optimization results we can see that the RV of cables can be effectively suppressed, the optimized parameters in TABLE 3 would be substituted into the system of Fig.3 to see whether the proposed method could control the RV of the moving platform, and the flexible displacement of the moving platform including the RV can be calculated as shown in Fig.7, for the point-to-point motion trajectory is only planned in X direction, the maximum RV in the corresponding direction plays the dominant role, which is about 5 times larger than the value in Y direction, while the RV in other direction is less than 0.006mm or rad and can be neglected in most applications. When one-order IS is adopted, the maximum RV is reduced from 0.173mm to 0.033mm, which means more than 80% RV is suppressed, and the value can be further reduced to 0.008mm and 0.003mm with two- and three-order IS, respectively, and the RV performance are also similar in Y, ϕ and θ direction, while the performance in Z and φ is not so ideal. There might be two reasons that can

account for this, the first reason is the RV in these two directions are neglected in the optimization for the value is relative too small, the second reason is the vibration frequencies in these two direction are of high order and the three-order IS is not enough for suppressing the corresponding RV, and which might be suppressed by high-order IS.

V. CONCLUSION

The dynamic modeling and RV suppression of the redundantly actuated CDPR were investigated in this paper. Unlike previous literature, the flexible displacement of the moving platform is treated as the generalized coordinates in the dynamic modeling for the convenience in RV suppression, and the deformation of cables are deduced under the generally accepted small deformation hypothesis, and with Newton-Euler equation the systematic level dynamic model were thus obtained. To suppress the RV for time-variant frequencies of the CDPR in point-to-point motion, the multiple-mode IS combined with the PSO and dynamic feedforward plus PD is proposed, and the feasibility of the method is elaborated. At last, the six-DOF CDPR with seven driving cables are taken as the example to validate the effectiveness of the proposed method, the simulation result show that the dominant RV can be effectively reduced, and the higher suppression accuracy for both the dominant and high-order RV can be obtained with the increase of the number of the IS at the cost of growing time delay.

REFERENCES

[1] Y. L. Kuo, W. L. Cleghorn, and K. Behdinan, "Stress-based finite element method for Euler-Bernoulli beams," *Trans. Can. Soc. Mech. Eng.*, vol. 30, no. 1, pp. 1–6, Mar. 2006.
[2] S. K. Dwivedy and P. Eberhard, "Dynamic analysis of flexible manipulators, a literature review," *Mechanism Mach. Theory*, vol. 41, no. 7, pp. 749–777, Jul. 2006.
[3] I. T. Pietsch, M. Krefft, O. T. Becker, C. C. Bier, and J. Hesselbach, "How to reach the dynamic limits of parallel robots? An autonomous control approach," *IEEE Trans. Autom. Sci. Eng.*, vol. 2, no. 4, pp. 369–380, Oct. 2005.
[4] J. Begey, L. Cuvillon, M. Lesellier, M. Gouttefarde, and J. Gangloff, "Dynamic control of parallel robots driven by flexible cables and actuated by position-controlled winches," *IEEE Trans. Robot.*, vol. 35, no. 1, pp. 286–293, Feb. 2019.
[5] H. J. Asl and F. Janabi-Sharifi, "Adaptive neural network control of cable-driven parallel robots with input saturation," *Eng. Appl. Artif. Intell.*, vol. 65, pp. 252–260, Oct. 2017.
[6] H. J. Asl and J. Yoon, "Robust trajectory tracking control of cable-driven parallel robots," *Nonlinear Dyn.*, vol. 89, no. 4, pp. 2769–2784, Sep. 2017.
[7] V. Ferravante, E. Riva, M. Taghavi, F. Braghin, and T. Bock, "Dynamic analysis of high precision construction cable-driven parallel robots," *Mechanism Mach. Theory*, vol. 135, pp. 54–64, May 2019.
[8] S. Baklouti, E. Courteille, P. Lemoine, and S. Caro, "Vibration reduction of cable-driven parallel robots through elasto-dynamic model-based control," *Mechanism Mach. Theory*, vol. 139, pp. 329–345, Sep. 2019.
[9] R. Qi, A. Khajepour, and W. W. Melek, "Generalized flexible hybrid cable-driven robot (HCDR): Modeling, control, and analysis," 2019, *arXiv:1911.06222*. [Online]. Available: http://arxiv.org/abs/1911.06222
[10] H. Jia, W. Shang, F. Xie, B. Zhang, and S. Cong, "Second-order sliding-mode-based synchronization control of cable-driven parallel robots," *IEEE/ASME Trans. Mechatronics*, vol. 25, no. 1, pp. 383–394, Feb. 2020.
[11] H. Wang, L. Shi, Z. Man, J. Zheng, S. Li, M. Yu, C. Jiang, H. Kong, and Z. Cao, "Continuous fast nonsingular terminal sliding mode control of automotive electronic throttle systems using finite-time exact observer," *IEEE Trans. Ind. Electron.*, vol. 65, no. 9, pp. 7160–7172, Sep. 2018.
[12] H. Jamshidifar, A. Khajepour, B. Fidan, and M. Rushton, "Vibration regulation of kinematically constrained cable-driven parallel robots with minimum number of actuators," *IEEE/ASME Trans. Mechatronics*, vol. 25, no. 1, pp. 21–31, Feb. 2020.
[13] R. de Rijk, M. Rushton, and A. Khajepour, "Out-of-plane vibration control of a planar cable-driven parallel robot," *IEEE/ASME Trans. Mechatronics*, vol. 23, no. 4, pp. 1684–1692, Aug. 2018.
[14] M. Rushton, H. Jamshidifar, and A. Khajepour, "Multiaxis reaction system (MARS) for vibration control of planar cable-driven parallel robots," *IEEE Trans. Robot.*, vol. 35, no. 4, pp. 1039–1046, Aug. 2019.
[15] H. Jamshidifar, S. Khosravani, B. Fidan, and A. Khajepour, "Vibration decoupled modeling and robust control of redundant cable-driven parallel robots," *IEEE/ASME Trans. Mechatronics*, vol. 23, no. 2, pp. 690–701, Apr. 2018.
[16] M. A. Khosravi and H. D. Taghirad, "Dynamic modeling and control of parallel robots with elastic cables: Singular perturbation approach," *IEEE Trans. Robot.*, vol. 30, no. 3, pp. 694–704, Jun. 2014.
[17] M. Shoaib, J. Cheong, D. Park, and C. Park, "Composite controller for antagonistic tendon driven joints with elastic tendons and its experimental verification," *IEEE Access*, vol. 6, pp. 5215–5226, 2018.
[18] R. J. Caverly and J. R. Forbes, "Flexible cable-driven parallel manipulator control: Maintaining positive cable tensions," *IEEE Trans. Control Syst. Technol.*, vol. 26, no. 5, pp. 1874–1883, Sep. 2018.
[19] R. J. Caverly and J. R. Forbes, "Dynamic modeling and noncollocated control of a flexible planar cable-driven manipulator," *IEEE Trans. Robot.*, vol. 30, no. 6, pp. 1386–1397, Dec. 2014.
[20] A. Abe, "Trajectory planning for residual vibration suppression of a two-link rigid-flexible manipulator considering large deformation," *Mechanism Mach. Theory*, vol. 44, no. 9, pp. 1627–1639, Sep. 2009.
[21] W. Singhose and J. Vaughan, "Reducing vibration by digital filtering and input shaping," *IEEE Trans. Control Syst. Technol.*, vol. 19, no. 6, pp. 1410–1420, Nov. 2011.
[22] W. Singhose, "Command shaping for flexible systems: A review of the first 50 years," *Int. J. Precis. Eng. Manuf.*, vol. 10, no. 4, pp. 153–168, Oct. 2009.
[23] M. J. Maghsoudi, Z. Mohamed, S. Sudin, S. Buyamin, H. I. Jaafar, and S. M. Ahmad, "An improved input shaping design for an efficient sway control of a nonlinear 3D overhead crane with friction," *Mech. Syst. Signal Process.*, vol. 92, pp. 364–378, Aug. 2017.
[24] Y. Liu, Y. Dong, and J. Tan, "Online-offline optimized motion profile for high-dynamic positioning of ultraprecision dual stage," *Complexity*, vol. 2018, pp. 1–13, Aug. 2018.
[25] J. M. Hyde, "Multiple mode vibration suppression in controlled flexible systems," M.S. thesis, Dept. Mech. Eng, Massachusetts Inst. Technol., Cambridge, MA, USA, 1991.

ZHENGSHENG CHEN was born in 1984. He received the Ph.D. degree in mechanical engineering from the Harbin Institute of Technology, China, in 2015. He is currently a Lecturer with the China University of Mining and Technology, China. His research interests include dynamic modeling, optimal design, and control of robotics.

XUESONG WANG (Member, IEEE) received the Ph.D. degree from the China University of Mining and Technology, in 2002. She is currently a Professor with the School of Information and Control Engineering, China University of Mining and Technology. Her main research interests include machine learning, bioinformatics, and artificial intelligence. She was a recipient of the New Century Excellent Talents in University from the Ministry of Education of China, in 2008. She is an Associate Editor of the IEEE TRANSACTIONS ON SYSTEMS, MAN, AND CYBERNETICS: SYSTEMS and the *International Journal of Machine Learning and Cybernetics*.